

# Investigation of Nanostructured Thin Films Adhesion used to Improve Tribological Characteristics of Hip Prostheses

L.L. Badita<sup>a</sup>, G. Gheorghe<sup>a</sup>, L. Capitanu<sup>b</sup>

<sup>a</sup>INCD-Mechatronics & Measurement Technique, 6-8 Pantelimon, District 2, 021631-Bucharest, Romania,

<sup>b</sup>Institute of Solid Mechanics of Romanian Academy, District 1, 010141-Bucharest, Romania.

## Keywords:

Hip prosthesis  
Thin films  
Nanostructures  
Adhesion  
Tribological properties

## ABSTRACT

Hip prosthesis is a complex mechanical biotribosystem with multiple functions. Under the action of cyclic dynamic loadings, developed in a biological adversely environment, it can lose the optimal functionality during the time. To improve mechanical characteristics of hip prostheses we deposited TiN films on SS316L steel substrates by pulse laser deposition method (PLD). Adhesion strength of the layer on the substrate was evaluated by scratch tests accompanied by different microscopy methods. Following these studies, we believe that the essential factor for increasing the hardness of femoral heads with thin layers is to provide a strong adherent coating to the substrate using PLD.

## Corresponding author:

Liliana - Laura Badita  
INCD-Mechatronics & Measurement  
Technique, 6-8 Pantelimon, District  
2, 021631-Bucharest, Romania  
E-mail: badita\_l@yahoo.com

© 2014 Published by Faculty of Engineering

## 1. INTRODUCTION

Endoprostheses surgery is a modern method for treatment of advanced stages of disease of the joints that gives the patient opportunity to avoid serious disability and return to active life. The surgery consists in regeneration using pseudo-implants of the fragments of joints destroyed by the disease.

Hip prosthesis is a complex mechanical biotribosystem with guiding, coupling, movement stopping and power transmission function. To restore the natural movement of the hip, total hip prosthesis consists of three elements [1]:

- an articular element (head of the prosthesis) determines the rotation center, axes and controls the articular movement. It has an important role in transmitting the forces, lubrication and wear of the prosthesis;
- a structural element (the central part of the prosthesis) that positions the articular element to the bone that it anchors. This element substitutes to intra-articular anatomy.
- an attachment element (the intramedullary stem) which is attached to the bone structure. This element is substituted to the intramedullary anatomy of the femoral duct.

Under the action of cyclic dynamic loadings and complex movements with six degrees of freedom, developed in a biological adversely environment, prostheses can lose the optimal functionality during the time. Thus, wear phenomena appear at the acetabular cup/femoral head interface manifesting itself in the deformation and wear of the acetabular cup, changing the surface roughness of the femoral head, the appearance of wear particles and their expulsion in synovial fluid, the appearance of three-body wear and rejection phenomenon [2]. So far, completely remove the problems associated with the use of hip prostheses, such as fracture and uncementing, physiological reactions of rejection and the most important – materials wear, failed. It was attempted the improvement of tribological performances through constructive changes and even the principle of operation [3]. Surface engineering offers the alternative possibility to reduce wear, wear particles production and release of ions in metal-metal couplings. Factors that could contribute to this reduction are: components durability increasing; a different surface chemistry to reduce adhesive friction; coated components that remain undamaged. During the years combinations of base materials have appeared from in vitro studies conducted by researchers and clinical data published in the literature [4-7]. The need to have resistant prostheses, with anticorrosive composition and improved mechanical properties led to the application of thin films of materials with superior properties on the prosthetic surfaces.

## 2. MATERIALS AND EXPERIMENTS

To obtain a more complete result about the durability of prostheses we have made thorough investigation of both components - the femoral head and acetabular cup.

At the end of these studies we proposed to find solutions for these shortcomings. We performed deposition of TiN thin films (nanomaterials) on SS316L cylindrical steel substrates to increase abrasion resistance [8].

### 2.1 TiN Deposition

TiN deposition was realized by physical laser deposition process inside a deposition chamber,

with stainless steel reaction chamber at 5000, 10000 and 20000 pulses.

PLD experiments were conducted using a KrF\* excimer source ( $\lambda = 248$  nm,  $\tau_{FWHM} = 25$  ns,  $\nu = 10$  Hz) – Fig. 1, running at a repetition frequency of 10 Hz. The laser beam was incident at  $45^\circ$  on the target surface.

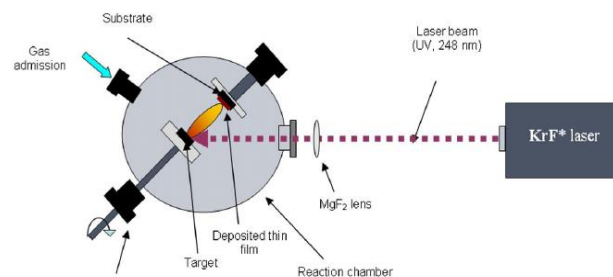


Fig. 1. PLD experimental scheme.

Thin commercial tablets (99.5 % purity, 1" diameter x 0.250" thick) were used as targets for experiments, while disks (cylindrical samples) made of SS 316L stainless steel (22.5 mm diameter and 10 mm height), hardness of 150 HV30 were used as substrates for deposition. Before deposition were heated and maintained at a constant temperature (500 °C).

All coatings were made in a dynamic flow of N<sub>2</sub> and the pressure inside the deposition chamber was  $\sim 2 \times 10^{-3}$  Torr. Microstructure of TiN coatings deposited by PLD was investigated using X-ray diffraction technique, by the courtesy of Sorin Moga and Denis Negrea from the University of Pitesti, Research Center for Advanced Materials.

### 2.2. Characterisation of deposited TiN layers

Microstructure of TiN coatings deposited by PLD was investigated using X-ray diffraction technique, by the courtesy of Sorin Moga and Denis Negrea from the University of Pitesti, Research Center for Advanced Materials. Diffraction measurements were performed with CuK $\alpha$  radiation on a system equipped with parallel optical and vertical  $\theta - \theta$  goniometer. Divergence angle of the beam emitted by the multilayer mirror is approximately  $0.05^\circ$ .

This optical type is suitable for thin films analysis, particularly for the measurements of residual stresses, due to the strong intensity of the beam and of the significant reduction of

instrumental errors (the position of the diffraction patterns is out of phase, the shape and the width of the diffraction lines profiles are maintained even at large angles of inclination) [10].

X-ray diffraction patterns are acquired at a fixed incidence angle  $\alpha = 1^\circ$ , in the angular range  $2\theta$  of  $34^\circ - 105^\circ$ , with the acquisition step of  $0.02^\circ$  and counting time per step of 10 s.

Microstructural analysis was performed using a specialized software package that allows Rietveld analysis of the full diffraction spectrum. Sections of SS316L steel samples, on which the layers were deposited, were made to determine the thickness of the TiN thin films deposited. The cross sections polished with sandpaper 400 and 600 were studied using optical microscopy (OM), atomic force microscopy (AFM) and scanning electron microscopy (SEM).

### 2.3. Scratching tests

Resistance of the substrate adhesion was evaluated by scratch tests accompanied by OM, AFM and SEM. By using scratch testing it is possible to prematurely detect the failure of TiN coating adhesion in real applications. Scratch testing method is a highly reproducible quantitative technique, in which the critical tasks where errors appear are used to compare the cohesion or adhesion properties of the coatings or of substrate material. During the test, on the sample are made scratches with a sphero-conical tip that is pulled at a constant speed over the sample, under a constant load.

The test was performed at room temperature ( $22^\circ\text{C}$ ), to better simulate the conditions whereat the coating is subjected to. Scratching process is simulated in a controlled and monitored approach, to observe the adhesive or cohesion failures. Times when the coating fails by deformation or breakage are taken as critical points of failure.

Specific parameters of the test include the loading speed (constant), scratching speed (1 cm/min), friction coefficient between the surface and indenter and internal stress in material.

Specific parameters of the sample for coating – substrate systems include the hardness and

roughness of the substrate, hardness and roughness of the coating, coating thicknesses.

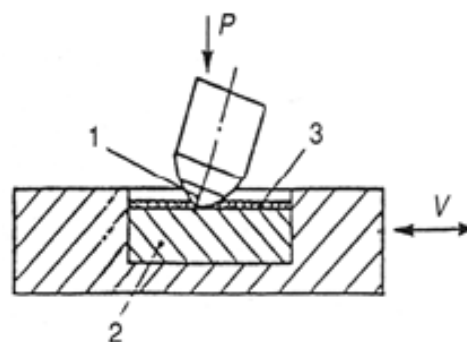
In our experiments, adhesion strength of TiN layers was analysed by making scratches with the tester presented in Fig. 2, with a spherical diamond tip, at loads of 2.5 N, 5 N, 10 N, 20 N, 40 N, 80 and 125 N.



(a)



(b)



(c)

**Fig. 2.** (a) Overview of scratch facilities with a diamond spherical segment. (b) View of the scratching thimble. (c) Functional scheme: 1 – natural diamond spherical segment; 2 – sample of tested material; 3 – lubricant.

Support plate of the testing sample (2) has an oscillatory motion. The sample is loaded by a spherical segment of diamond, with a radius of 2 mm (1). The plate is coated with a thin layer (3) of lubricant (bovine serum) during the test. Use of a friction thimble involving natural diamond against the material to be investigated, allows to considerably simplify the testing devices, the movement being sliding motion.

Microscopic observation is the most reliable method to detect surface damage. This technique is able to differentiate between cohesive failure of the coating and adhesive failure at the interface of the coating – substrate system. Usually, a sample failure will lead to a change of the friction coefficient. Abrupt change of the depth data may indicate delamination. Also, information about depth, pre and post scratching, can give information on the plastic deformation towards the elastic one, during the test.

### 3. RESULTS

#### 3.1. Physical characterization of deposited TiN layers

Physical characterization of deposited TiN layers was performed by Fourier Transform Infrared Spectroscopy (FTIR), AFM and OM. Following FTIR investigations the existence of an N-H bond has been demonstrated. Thus, this analysis can demonstrate the stoichiometric transfer of material, i.e., deposition of TiN layer.

Topographic parameters determined by the AFM (roughness  $R_a$ , maximum height  $h_{max}$ , 10 point height  $R_z$ , surface skewness  $R_{sk}$ , coefficient of kurtosis  $R_{ka}$ ) provide information on the distribution of the deposited layer, resulting that under the deposition there is a more veiled area.

#### 3.2. The thickness and hardness of deposited TiN layers

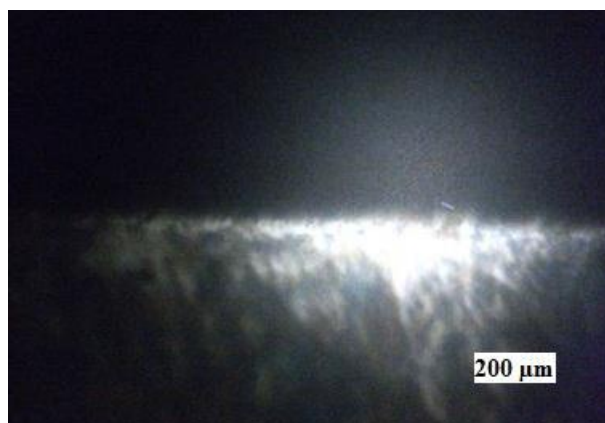
The thickness and hardness of deposited TiN layers are very important for their quality. Therefore, before investigations the adhesion of TiN nanostructured thin films, we determined these parameters using different methods (OM, AFM and SEM).

Few images obtained after the microscopic analysis are presented in Fig. 3a and 3b. The existence of material layer deposited on the steel surface, and also a diffusion of the layer deposited in the substrate can be observed. This is seen more clearly in the case of samples with layer deposited at 20000 pulses.

Images obtained by OM shown in Fig. 3, somewhat less clear due to light reflected by the ground slide were inspected as images, and with help of AFM software to determine the thickness of deposited thin layers. Images obtained by OM shown in Fig. 3, somewhat less clear due to light reflected by the ground slide were inspected as images, and with the help of AFM software to determine the thickness of deposited TiN layers.



(a)

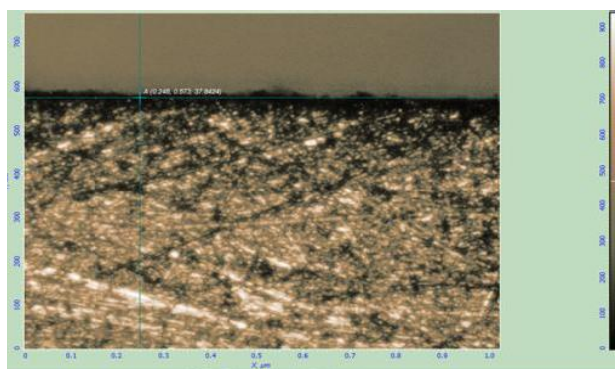


(b)

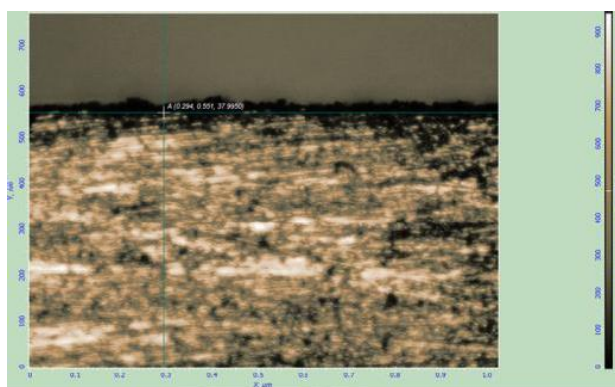
**Fig. 3.** Analysis by optical microscopy of cross sections of the samples coated with TiN: (a) 5000 and (b) 20000 pulses (magnification 1000x).

We tried to determine the thickness of the TiN layers deposited at 5000, 10000 and 20000 pulses by scanning its surfaces with AFM (few examples in Fig. 4).

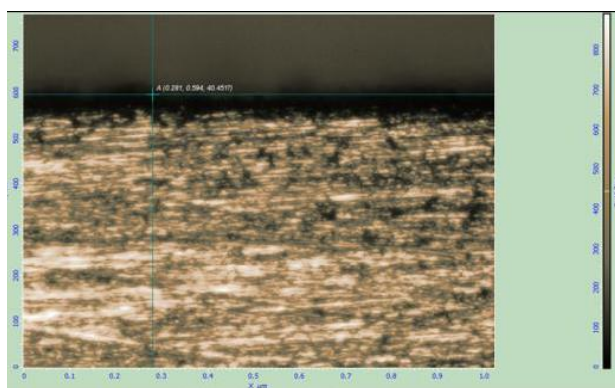




(a) 5000 pls<sub>10</sub> → 1.5 μm



(b) 10000 pls<sub>1</sub> → 1.9 μm



(c) 20000 pls<sub>9</sub> → 4.1 μm

**Fig. 4.** AFM study of cross sections of stainless steel samples coated with TiN at (a) 5000 pulses, (b) 10000 pulses and (c) 20000 pulses.

For precision, measurements of thickness were also realized by SEM, at different magnifications (250X, 1000X and 2000X).

As a result, the average thickness of deposited layers determined by different methods is:

- by OM: 1,1 μm for 5000 pulses and 1,62 μm for 20000 pulses;
- by AFM: 1,67 μm for 5000 pulses, 2,11 μm for 10000 pulses and 2,72 μm for 20000 pulses;

- by SEM: 0,8 – 1 μm for 5000 pulses, 1,2 – 1,4 μm for 10000 pulses and 1,5 – 1,6 μm for 20000 pulses.

This is manifested by an increase in hardness of layer-substrate composite with increasing the layers thickness.

The measurements performed had as result the hardness values of SS316L steel samples before coating and the microhardness of TiN layers deposited. Average hardness values are presented in Table 1.

**Table 1.** Hardness of layer and substrate of the used samples.

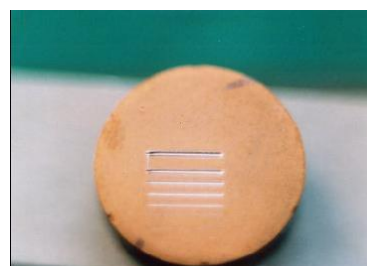
Sample	Hardness of the layer Micro HV 50 gf	Hardness of the substrate Micro HV 50 gf
5 k	349	287
10 k	539	420
20 k	738	467

Hardness is higher for the TiN layer than the initial hardness of the substrate.

An increase of the layers thickness and appropriate of the composite hardness with the increase of pulses number were observed. Thus, it is possible that the uniformity of deposited layers to occur after the coating with a thicker layer of the defects existing in the substrate (with a higher thickness for 2000 pulses sample).

### 3.3. Investigations of the TiN layers surfaces scratch tested using OM

All TiN layers deposited at 5000, 10000, 20000 pulses were scratch tested (Fig. 5) and, subsequently, surfaces of steel SS316L disks coated with TiN were macroscopically and microscopically studied.



(a)



(b)



(c)

**Fig. 5.** Macroscopic image of the SS 316L steel sample coated with TiN at (a) 5000 pulses, (b) 10000 pulses and (c) pulses after scratch tests

Several types of surfaces damages (main critical events - Ec) occurring after the critical loads action were detected after scratch testing on each sample and examining scratch traces using OM: material deformations and detachments

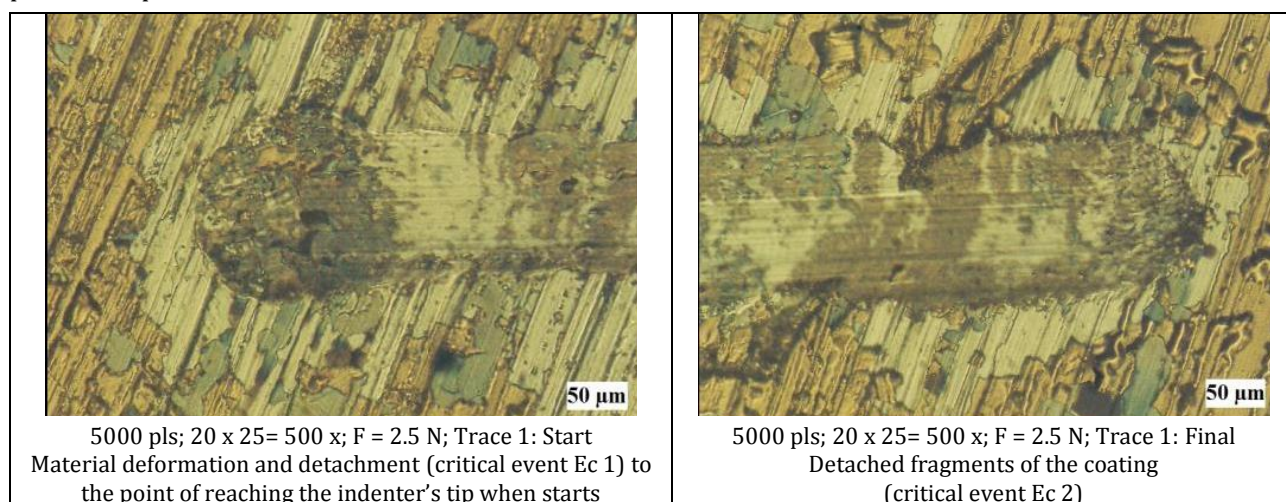
(Ec1), detached fragments of the coating (Ec2), semicircular cracks of the coating (Ec3), raising material on the edges (Ec4), chipping the base material (Ec5) and oxidation (Ec6). In Table 2 there is a summary of information about the main features of scratches made on the surface of TiN coating deposited with 5000 pulses after the scratch test. It is about the critical events that occur in certain moments of critical forces action, with values of 2.5 N, 5 N, 10 N, 20 N, 40 N and 80 N. A part of the microscopic images of the traces appeared after the scratch tests performed, i.e. those that correspond to the critical events are presented in Table 3.

In Table 4 is the information about the main features of scratches made on the surface of TiN coating deposited with 10000 pulses after the scratch test. It is about critical events that occur in certain moment of critical forces action, with values of 2.5 N, 5 N, 10 N, 20 N and 80 N. Microscopic images of the traces occurred after the scratch tests performed are presented in Table 5.

**Table 2.** Main characteristics of the TiN layer surface deposited with 5000 pulses, after scratch tests.

No	Magnification	Critical load	Trace	Place on the trace	Observations
1	25x20=500x	Fc1	1	Start	Material deformations and detachments (critical event Ec1) to the point of reaching the indenter's tip when starts
2	25x20=500x	Fc2	1	Final	Detached fragments of the coating (critical event Ec2) 3.5 mm
3	25x20=500x	Fc3	1	Pathway	Semicircular crack (critical event Ec3) 1 mm
4	25x20=500x	Fc4	3	Pathway	Raising material on the edge starts (critical event Ec4)
5	25x20=500x	Fc5	4	Start	Chipping the base material starts (critical event Ec5)

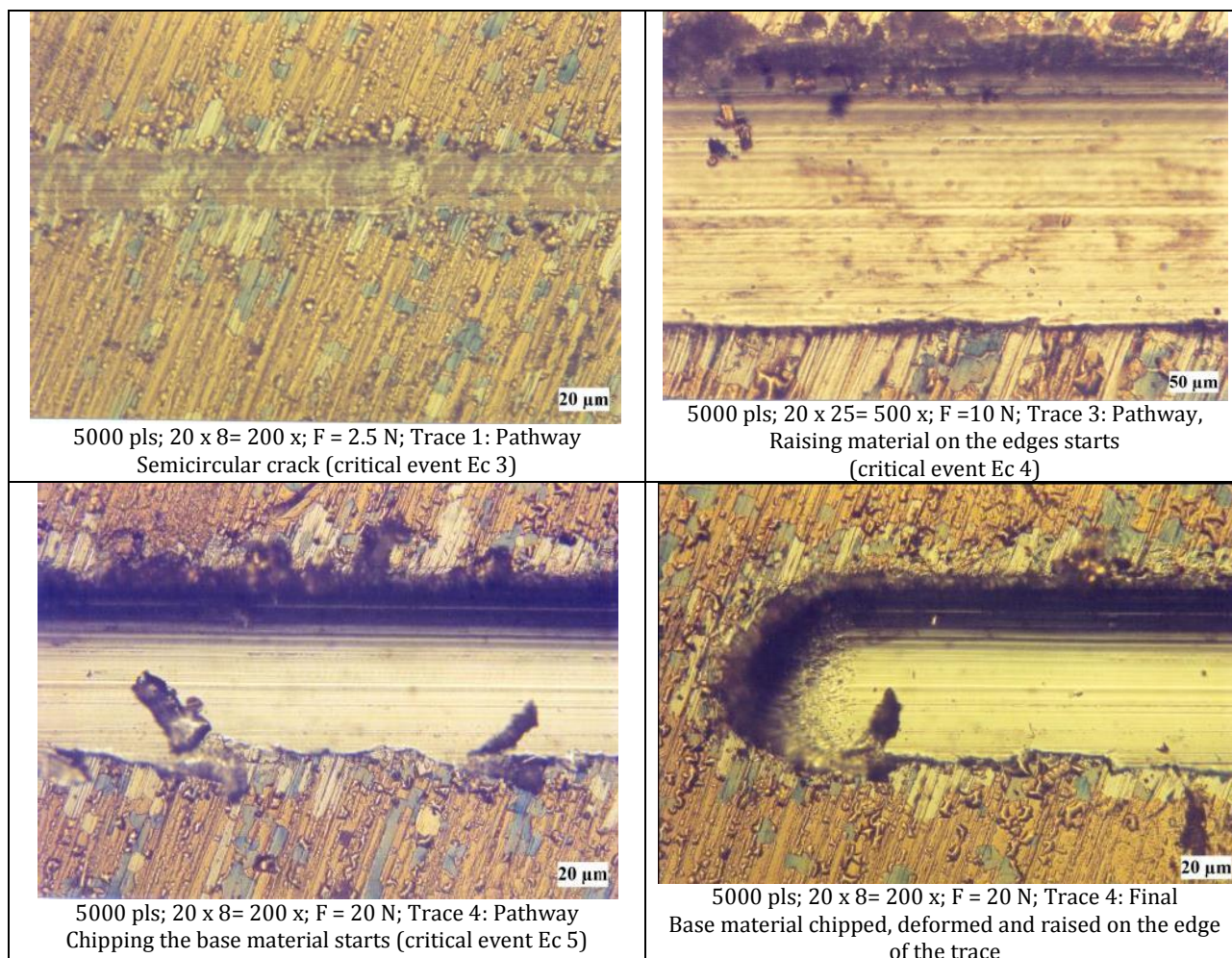
**Table 3.** Microscopic images of the main critical events appeared after scratch tests on the surfaces of 5000 pulses sample.



5000 pls; 20 x 25= 500 x; F = 2.5 N; Trace 1: Start  
Material deformation and detachment (critical event Ec 1) to the point of reaching the indenter's tip when starts

5000 pls; 20 x 25= 500 x; F = 2.5 N; Trace 1: Final  
Detached fragments of the coating (critical event Ec 2)






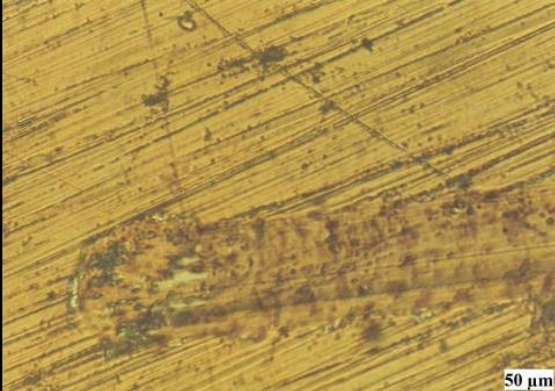
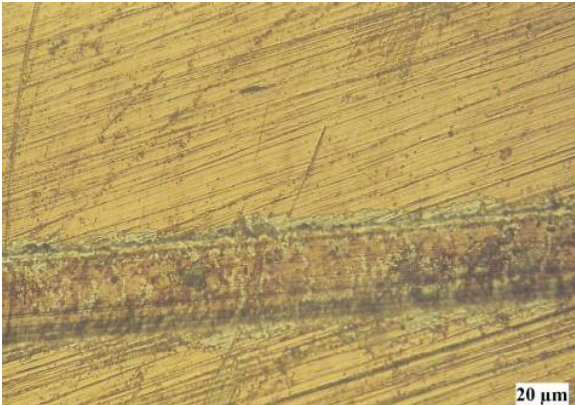

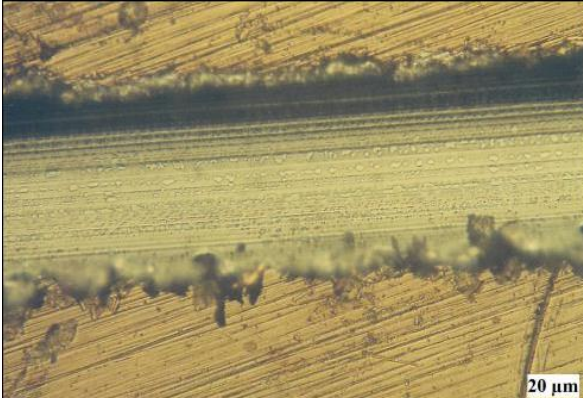
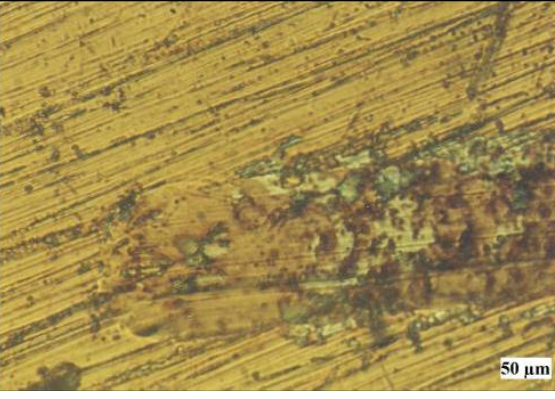
**Table 4.** Main Characteristics of the TiN layer surface deposited with 10000 pulses, after scratch test.

No	Magnification	Critical load	Trace	Place on the trace	Observations
1	25x8=200x	Fc1	1	Start	Material initial deformations and detachments (critical event Ec1) to the point of reaching the indrnter's tip when starts
2	25x8=200x	Fc3	1	Final	Detached fragments of the coating (critical event Ec2)
3	25x8=200x	Fc6	2	Start	Oxidation traces (critical event Ec6)
4	25x8=200x	Fc3, Fc2	3	Pathway	Semicircular crack (critical event Ec3) and detached deposition fragments (critical event Ec2)
5	25x8=200x	Fc4	5	Pathway	Raising material on the edge starts (critical event Ec4)
6	25x8=200x	Fc5, Fc6	5	Pathway	Chipping the base material starts (critical event Ec5) and raising material on the edge starts (critical event Ec4)

Ec – critical event; Fc – critical force; trace 1 = 2.5 N; trace 2 = 5 N; trace 3 = 10 N; trace 4 = 20 N; tace 5 = 40 N; trace 6 = 80 N



**Table 5.** Microscopic images of the main critical events appeared after scratch tests on the surfaces of 10000 pulses sample.

 <p>20 <math>\mu</math>m</p>	 <p>50 <math>\mu</math>m</p>
<p>10000 pls; 25 x 8= 200 x; F = 2.5 N; Trace 1: Start Material deformation and detachment (critical event Ec 1) to the point of reaching the indenter's tip when starts</p>	<p>5000 pls; 20 x 25= 500 x; F = 2.5 N; Trace 1: Final Detached fragments of the coating (critical event Ec 2)</p>
 <p>20 <math>\mu</math>m</p>	 <p>20 <math>\mu</math>m</p>
<p>10000 pls; 20 x 8= 200 x; F = 10 N; Trace 3: Pathway Semicircular crack (critical event Ec 3)</p>	<p>10000 pls; 25 x 8= 300 x; F =40 N; Trace 5: Start Raising material on the edges starts (critical event Ec 4)</p>
 <p>20 <math>\mu</math>m</p>	 <p>50 <math>\mu</math>m</p>
<p>10000 pls; 25 x 8= 200 x; F = 40 N; Trace 5: Pathway Chipping the base material starts (critical event Ec 5)</p>	<p>10000 pls; 25 x 20= 500 x; F = 5 N; Trace 2: Start Oxidation traces (critical event Ec 6)</p>

In Table 6 is a summary of the information about the main features of scratches made on the surface of TiN coating deposited with 20000 pulses after the scratch test. It is about the critical events that occur in certain

moments of critical forces action, with values of 2.5 N, 5 N, 10 N, 20 N, 40 N, 80 N and 125 N. Microscopic images of the traces occurred after the scratch tests performed are presented in Table 7.


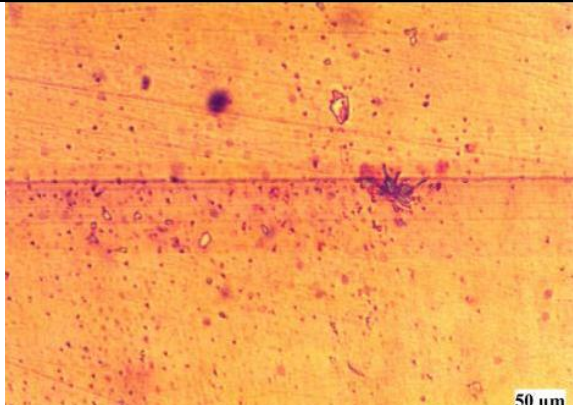
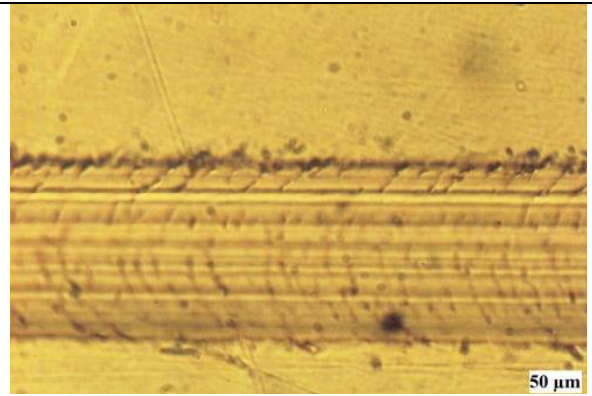
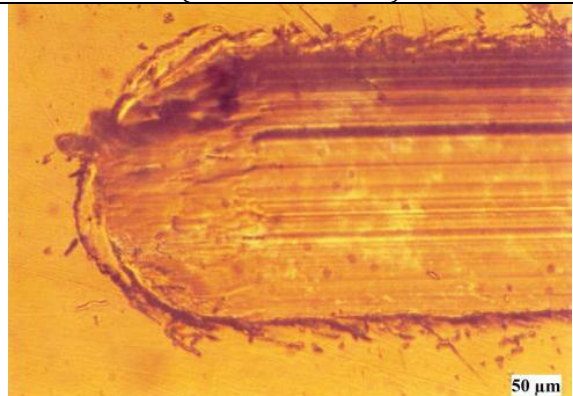


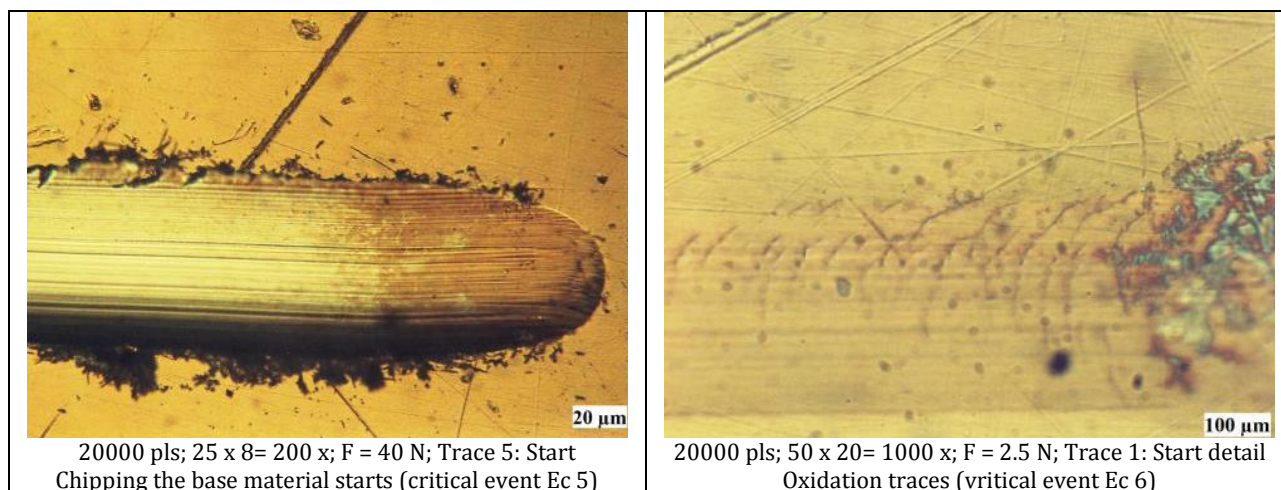
**Table 6.** Main Characteristics of the TiN layer surface deposited with 20000 pulses, after scratch test.

No	Magnification	Critical load	Trace	Place on the trace	Observations
1	25x20=500x	Fc3, Fc6	1	Start	Semicircular cracks (critical event Ec3) and oxidation traces (critical event Ec6) to the point of reaching the indenter's tip when starts
2	25x20=500x	Fc1, Fc6	1	Final	Material initial deformations and detachments (critical event Ec1) to the point of reaching the indenter's tip when starts and oxidation traces (critical event Ec6)
3	25x20=500x	Fc2	1	Pathway	Detached fragments of the coating (critical event Ec2)
4	25x20=500x	Fc4	4	Final	Raising material on the edge starts (critical event Ec4)
6	25x8=200x	Fc5	5	Start	Chipping the base material starts (critical event Ec5) and raising material on the edge starts (critical event Ec4)

Ec – critical event; Fc – critical force; trace 1 = 2.5 N; trace 2 = 5 N; trace 3 = 10 N; trace 4 = 20 N; tace 5 = 40 N; trace 6 = 80 N; trace 7 = 125 N

**Table 7.** Microscopic images of the main critical events appeared after scratch tests on the surfaces of 20000 pukes sample.

	
<p>20000 pls; 25 x 20= 500 x; F = 2.5 N; Trace 1: Final Material initial deformation and detachment (critical event Ec 1)</p>	<p>20000 pls; 25 x 20= 500 x; F = 2.5 N; Trace 1: Final Detached fragments of the coating (critical event Ec 2)</p>
	
<p>20000 pls; 25 x 20= 500 x; F = 10 N; Trace 3: Pathway, Semicircular crack (critical event Ec 3)</p>	<p>20000 pls; 25 x 20= 500 x; F =20 N; Trace 4: Final Raising material on the edges starts (critical event Ec 4)</p>



**Table 8.** Average roughness values of the three samples coated with TiN at 5000, 10000 and 20000 pulses.

No. trace	Force (N)	Average roughness (nm)		
		5000 pulses	10000 pulses	20000 pulses
1	2.5	34,569	42,309	16,591
2	5	35,095	57,695	21,063
3	10	42,309	65,778	80,354
4	20	47,387	65,680	98,104
5	40	87,293	92,447	115,325
6	80	-	79,277	83,599
7	125	-	-	56,932

It can be observed that on all 3 layers deposited at 5000, 10000 and 20000 pulses, critical events such as Ec1, Ec2, Ec3, and Ec6 occur depending on the layer's thickness since the action of forces with low values. Critical events Ec4 and Ec5 appear at higher values of force for the layers deposited at 10000 and 20000 pulses. This demonstrates higher hardness of these layers compared to the one deposited at 5000 pulses.

### 3.4. Investigations of the TiN layers surfaces scratch tested using AFM

For a more complete characterization of surfaces coated with TiN after the scratch tests, their characterization using AFM was also performed. Topographic parameters (roughness  $Ra$ , maximum height  $h_{max}$ , ten point height  $Rz$ , surface skewness  $Rsk$ , and coefficient of kurtosis  $Rkq$ ) determined by AFM study of TiN layers surfaces after the scratch test provides information on their distribution. AFM scans were performed on deposited TiN coatings, but scratches obtained after applying a force greater than 40 N on the layer deposited at 5000 pulses could not be scanned properly.

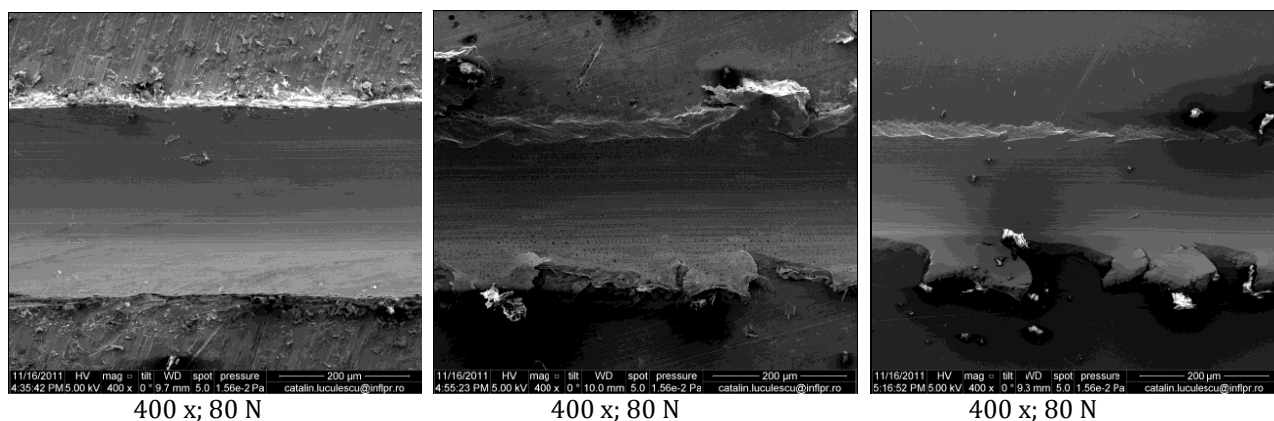
Analyzing the average roughness (Table 8) an increase in its value with increasing the applied force is observed. This may be due to the fact that with increasing force, scratches present different depths and for certain values a peeling of the layer occurs (and hence the layer's non-uniformity increases). The scratch test also affected the substrate due to peeling of the coating at certain values of force and only for certain layers.

For deposited layers a decrease in average roughness values is generally seen, so 5000 pulses → 10000 pulses → 20000 pulses. Alternating increase and decrease of roughness values of these measurements is due to non-uniform deposition of the layer.

### 3.5. Investigations of the TiN layers surfaces scratch tested using SEM

For a more accurate characterization of surfaces of TiN thin films subjected to scratch tests were also performed their SEM investigations. An example is shown in Fig. 6, where it can be seen that the same amount of force, the surface of TiN is harder with increasing number of pulses used at deposition.





**Fig. 6.** SEM images of the surfaces of TiN layers deposited at 5000, 10000 and 20000 pulses after the scratch test with 80 N (magnification 400x).

### 3.6. Determining of width and depth of the scratches drawn on the surfaces of TiN coatings after the scratch tests

On the images obtained by OM, the widths of scratch traces were measured. Average values are shown in Tables 9-11, then their depths  $h$

were calculated (Table 9, Table 10, Table 11) based on a simplified relationship (indent method), which takes into account the radius of diamond tip ( $r$ ) and mean value of the measured widths of the scratch ( $l$ ):  $h = 12/8r$ . In this case the radius of diamond tip is 2 mm.

**Table 9.** Widths and depths values of the scratch traces for the 5000 pulses sample.

No.	Magnification	Trace	Place	Number of divisions	Division value	$h$ (µm)
2.	200 x	1	Pathway	5	0.01	0.00625
8.	200 x	2	Pathway	6	0.012	0.00900
13.	200 x	3	Start	9	0.018	0.02025
20.	200 x	4	Pathway	12	0.024	0.03600
25.	200 x	5	Pathway	14	0.028	0.04900
28.	500 x	6	Final	15	0.075	0.35150

Tin / SS 316L; HV<sub>0.05</sub> / HV<sub>5</sub> = 349 / 287

**Table 10.** Widths and depths values of the scratch traces for the 10000 pulses sample.

No.	Magnification	Trace	Place	Number of divisions	Division value	$h$ (µm)
2.	200 x	1	Final	3	0.006	0.00225
8.	200 x	2	Pathway	5	0.010	0.00625
13.	200 x	3	Pathway	7	0.014	0.01225
20.	200 x	4	Pathway	10	0.020	0.02500
25.	200 x	5	Pathway	13	0.026	0.04225
29.	500 x	6	Pathway	15	0.030	0.05625

Tin / SS 316L; HV<sub>0.05</sub> / HV<sub>5</sub> = 349 / 287

**Table 11.** Widths and depths values of the scratch traces for the 20000 pulses sample.

No.	Magnification	Trace	Place	Number of divisions	Division value	$h$ (µm)
2.	200 x	1	Pathway	7	0.014	0.01225
8.	200 x	2	Pathway	12	0.024	0.03600
11.	200 x	3	Pathway	15	0.030	0.05625
17.	200 x	4	Pathway	23	0.046	0.13225
23.	200 x	5	Pathway	26	0.052	0.16900
29.	200 x	6	Pathway	28	0.056	0.19600
26.	200 x	7	Pathway	29	0.058	0.21025

Tin / SS 316L; HV<sub>0.05</sub> / HV<sub>5</sub> = 349 / 287

Graphic variation curves of scratch depth depending on the applied normal load were drawn considering the depth of obtained scratches (Figs. 7-9). These curves show some drops due to various defects of the coating.

It can be seen from these images that at a certain value, the layer is removed during the scratch test. The force applied whereat the deposited layer is removed from the substrate defines the critical force (load) (Fc). This is influenced by many factors, like substrate hardness, film thickness, interface contact and the intrinsic properties of the deposited film.

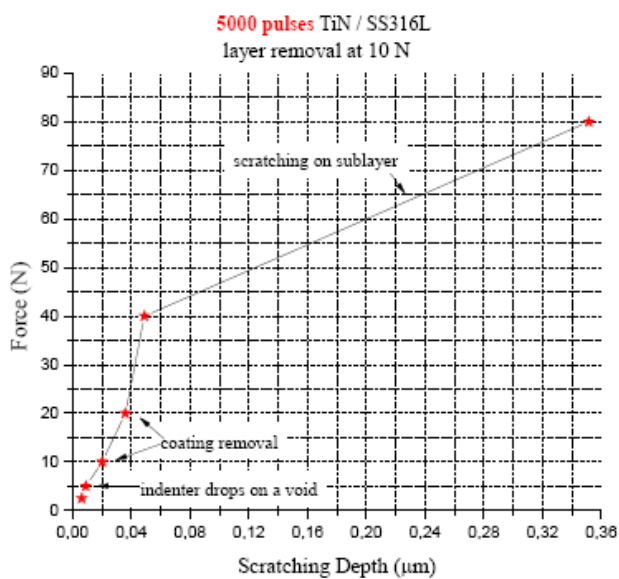


Fig. 7. Force - depth diagram for deposited layer at 5000 pulses.

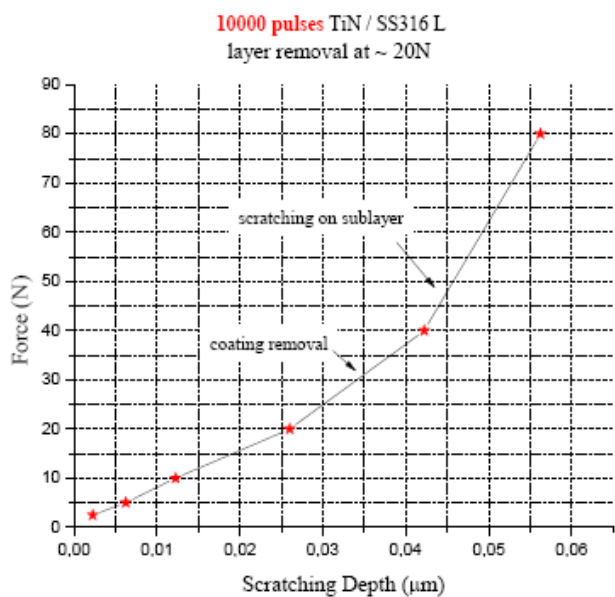


Fig. 8. Force - depth diagram for deposited layer at 10000 pulses.

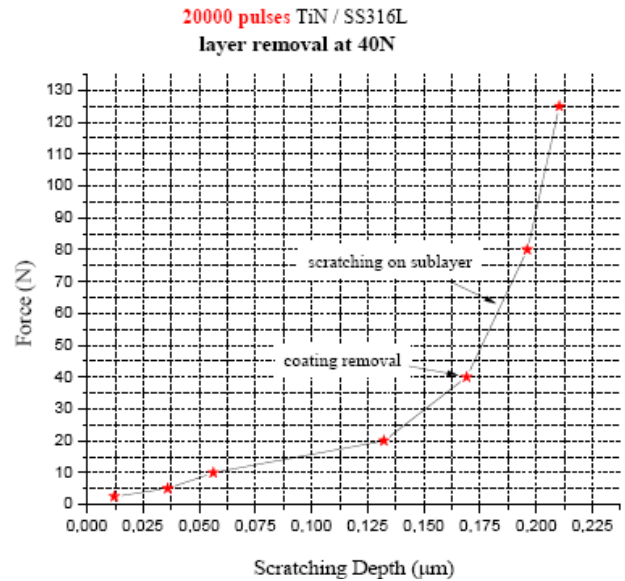


Fig. 9. Force - depth diagram for deposited layer at 20000 pulses.

The value of critical force is affected by different testing parameters (scratching speed, tip properties, etc.) and the coating-substrate composite properties (hardness and roughness of the surface, etc.).

When the layer is removed, the substrate's destruction was observed along the main scratch when the applied force is higher. The depths of the scratches obtained are different depending on the force values.

Figure 10 presents a comparative diagram between the three deposited layers. One can easily observe that the films deposited with 5000 pulses and 10000 pulses cannot support a force greater than 80 N.

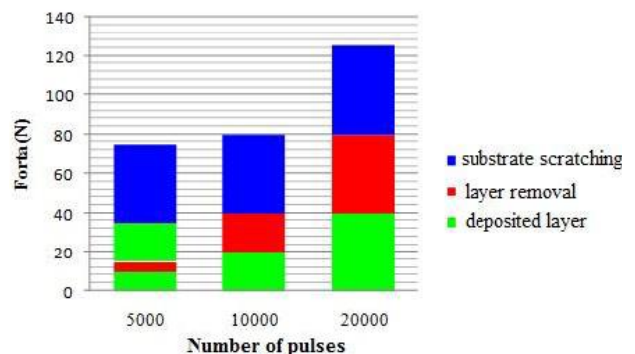


Fig. 10. Comparative force - number of pulses diagram of the three layers applied.

The layer deposited at 20000 pulses can also resist when on its surface a force of 125 N is applied during the scratching test. Force



whereat deposited layer removing begins increases with the number of pulses that is used to deposit the layer: 10 N for the sample with the layer deposited at 5000 pulses, 20 N for the sample with the layer deposited at 10000 pulses and 40 N for the sample with the layer deposited at 20000 pulses. Layer removal is accomplished within an increasingly larger range, for the 5000 pulses sample being necessary to apply a force of 10 N and increase with only 10 N to complete the removal. For 10000 pulses sample the substrate removal starts when a 20 N force is applied, and an increase of 20 N determines the completion of this process. A force of 40 N with an increase of another 40 N can remove the layer from the sample of 20000 pulses.

These results confirm the studies realized by other authors [11-13], who have reported the linear increase of critical load with the substrate hardness. In the measurements of these tests, layer deposited at 20000pulses has the highest hardness.

A force of 40 N determines the start of the scratching process of the substrate for 5000 and 10000 pulses samples. At this value of force, for the sample with layer deposited at 20000 pulses, the layer removal just starts. Thus, it can be seen that this sample is a stronger layer, possibly a stronger adhesion of the layer compared to the other two samples. The range necessary for scratching the substrate is greater for 20000 pulses sample with 5 N from the first two samples, where is necessary to increase the force from 40 N to 80 N.

An important conclusion that can be drawn from these observations is that the layer deposited at 20000 pulses is stronger, more adherent to the substrate and more uniformly deposited than the other two samples.

#### **4. CONCLUSION**

At depositions, the deposited nanostructured TiN material diffused in the base material. Thus, an important conclusion and also a novelty refers to the fact that the layer is more inclusive, that would be useful the sputtering deposition of an intermediate Ti layer (which diffuses into steel) and after this the deposition of final TiN layer. Processing, the treatment of substrate and

its roughness, together with PLD coating technological parameters must be chosen in order to facilitate the establishment of double diffusion of the interlayer between the layer and the substrate. The thickness of the deposited layer is non-uniform due to initial surface and a non-uniform roughness of the substrate.

We believe that the essential factor to increase femoral heads durability with thin layers is to provide a strong adherent coating to the substrate. This is a problem that belongs to the substrate's surface processing, and also to the coating process parameters.

Results obtained in this work after the scratch tests and after the depth of the scratch depending on the force applied diagram, for SS 316L steel coated with TiN lead to the conclusion that PLD could be a solution.

It should be noted that TiN coatings deposited by the PLD technique with the maximum number of pulses (20000 pulses) may be an alternative technology to ensure adhesion and scratch resistance of TiN coatings on femoral heads made of Ti-6Al-4V. It is possible that one of the causes to loss the adherence is the lack of an elastic modulus suitable to the mechanical characteristics of the coating and the substrate. The condition for the success of such coating is to provide an optimal surface roughness of the femoral head, which serves as support for TiN layer.

Overall analysis of experimental results, it can be concluded that although the layer of 20000 pulses is promising as alternative technology, further study is needed to determine the optimal roughness of the base layer, compatibilization with the hardness and determination of the optimum ratio between layer's elasticity and substrate's elasticity. Perhaps that will be necessary adhesion and biocompatibility studies of TiN structure by this method.

#### **Acknowledgement**

The authors would like to thank the National Institute of Research and Development in Mechatronics and Measurement Technique Bucharest and Romanian Academy, for its material and technical support offered in order to achieve these researches.

## REFERENCES

- [1] M. Popescu, L. Capitanu: *Ortopedics and Engineering* (in Romanian), Bren Publishing House, Bucharest, 2006.
- [2] L. Capitanu, L.L. Badita, D.C. Bursuc: *About damage of femoral head of total hip prosthesis*, Journal of the Balkan Tribological Association, Vol. 190, No. 2, pp. 155-161, 1995.
- [3] L. Capitanu, L.L. Badita: *Total Hip arthroplasty: Dynamic of Stability Loosening of Total Hip Prostheses* (in Romanian), AGIR Publishing House, Bucharest, 2011.
- [4] B. Cales: *Zirconia as a sliding material: histologic, laboratory, and clinical data*, Clin Orthop Relat Res., Vol. 379, pp. 94-112, 2000.
- [5] H. Migaud, A. Jobin, C. Chantelot, F. Giraud, P. Laffargue, A. Duquenois: *Cementless Metal – on metal Hip Arthroplasty in Patients Less Than 50 Years of Age. Comparison with Matched Control Group Using Ceramic – on Polyethylene after a Minimum 5-Year Follow-Up*, The Journal of Arthroplasty, Vol. 19, No. 8, pp. 23-28, 2004.
- [6] M.T. Clarke, P.T. Lee, R.N. Villar: *Numerical characterization of wear particle morphology*, in: I.M. Hutchings (Ed.): *New Directions in Tribology*, Mechanical Engineering Publications Ltd., Bury St Edmunds, pp. 371-389, 1997.
- [7] D. Dowson, C. Hardaker, G.H. Issac: *A Hip Joint Simulator of the Performance of Metal on Metal Joints. Part I: The Role of Materials*, The Journal of Arthroplasty, Vol. 19, No. 8, pp. 118-123, 2004.
- [8] G. Gheorghe, L.L. Badita: *Improving Tribological Characteristics of Hip Prosthesis Using Biocompatible Nanocoatings*, Advanced Materials Research, Vol. 741, pp. 67-72, 2013.
- [9] G. Socol, A.C. Galca, C.R. Luculescu, A. Stanculescu, N. Stefan, E. Axente, L. Duta, C.M. Mihailescu, V. Craciun, D. Craciun, V. Sava, I.N. Mihailescu: *Tailoring of Optical, Compositional and Electrical Properties of the  $In_xZn_{1-x}O$  Thin Films Obtained by Combinatorial Pulses Laser Deposition*, Digest J. of Nanomaterials and Biostructures, Vol. 6, pp. 107 – 115, 2011.
- [10] A. Kumar, U. Weltzel, E.J. Mittelmeijer: *Diffraction Stress Analysis of Strongly Fibre – Textured Gold Layers*, J. Kristallografie Suppl, Vol. 23, pp. 55-60, 2006.
- [11] A.J. Perry: *Scratch adhesion testing of hard coatings*, Thin Solid Films, Vol. 107, No. 2, pp. 167-180, 1983.
- [12] P.A. Stainmann, H.E. Nintermann: *Adhesion of TiC and Ti(C,N) coatings on steel*, J. Vac. Sci. Technol., Vol. 3, No. 6, pp. 2394-2400, 1985.
- [13] H. Ichimura, A. Rodrigo: *The correlation of scratch adhesion with composite hardness for TiN coatings*, Surf. Coat. Technol., Vol. 126, No. 2-3, pp. 152-158, 2000.